Key Points:
- Using 25-year rawinsonde observations, we report on the boundary layer depth variability over 18 coastal sites in the contiguous United States
- Striking differences emerged in the boundary layer depths due to interplay between marine air mass and continental air mass
- The offshore versus onshore contrasts in the boundary layer depths vary both seasonally and spatially among the coastal regions

Supporting Information:
- Supporting Information S1

Correspondence to:
S. Pal,
sandip.pal@ttu.edu

Contrasting Air Mass Advection Explains Significant Differences in Boundary Layer Depth Seasonal Cycles Under Onshore Versus Offshore Flows

Sandip Pal[1] [ID] and Temple R. Lee[2,3] [ID]

[1]Department of Geosciences, Atmospheric Science Division, Texas Tech University, Lubbock, TX, USA, [2]Cooperative Institute for Mesoscale Meteorological Studies (CIMMS), Norman, OK, USA, [3]Atmospheric Turbulence and Diffusion Division, Air Resources Laboratory, NOAA, Oak Ridge, TN, USA

Abstract The complexities in the atmospheric boundary layer depth (BLD) features over coastal regions pose challenges for meteorological forecasts, air quality, greenhouse gas mixing and transport, and wind energy production. Here, for the first time, we investigated afternoon BLD variability over 18 coastal sites in the contiguous United States located along the Gulf of Mexico, Atlantic Ocean, and Pacific Ocean using 25 years of rawinsonde launches. Due to influence of shallow marine layer air via onshore flow, substantially large BLD contrasts (ΔBLD, BLD under offshore minus onshore) were found. ΔBLDs over the sites varied both seasonally and spatially among the coastal regions and within a region. For the sites along the Gulf of Mexico and Atlantic Ocean, ΔBLDs were found to be higher in spring and summer (500–1,500 m) than in winter and fall (100–450 m). Results underscore the importance of advection on BLD footprints and provide observational constraints for model evaluation.

Plain Language Summary The depth of the Earth's atmospheric boundary layer is an important parameter that atmospheric scientists use in weather forecast models and for understanding the height to which pollutants emitted from Earth's surface are mixed into the atmosphere. In our study, we investigated how the depth of the boundary layer varied at coastal sites along the Gulf of Mexico, Atlantic Ocean, and Pacific Ocean using 25 years of boundary layer depths obtained using weather balloon launches. We found large differences in boundary layer depths that depended on whether the wind was blowing onshore or offshore. Offshore winds resulted in much deeper boundary layers than onshore winds. The difference between boundary layer depths when the wind was offshore versus onshore was largest during the spring and summer at sites located along the Gulf of Mexico and Atlantic Ocean.

1. Introduction

A detailed understanding of the atmospheric boundary layer (ABL) and accurate representation in numerical simulations is critical for meteorological forecasts, air quality forecasts, greenhouse gas transport (e.g., Behrendt et al., 2005; Medeiros et al., 2005; Stull, 1988), and climate forcing (Davy & Esau, 2016). Atmospheric processes that impact coastal regions are critical due to frequent air mass interactions between land and sea yielding quasi-regular onshore and offshore flows. The orientation, topography, and surface properties, and ABL structure over coastlines make transport processes more complex, posing additional challenges to numerical models (e.g., Marshall et al., 2004).

Marine transportation facilities, economic growth, urbanization, and sufficient resources for recreation are some of the reasons why coastal areas worldwide are rapidly becoming home to more than 40% of the world's population (Neumann et al., 2015). Since coastal areas around the world are becoming potential locations for deploying wind turbines, detailed knowledge of ABL features under offshore and onshore flows is important for optimizing the efficiency of wind farms (Pichugina et al., 2012). A better understanding of the transport of pollutants, in particular health-hazardous aerosols, trace gases, greenhouse gases, and their exchange with the free troposphere above the top of ABL in coastal areas is essential for regional air quality and climate studies. Coastal areas are significantly affected by differential heating, which generate quasi-regular land and sea breezes. These land and sea breezes, combined with complexities in the coastal topography, generate complexities in the thermodynamic features of the ABL, in particular, the boundary layer depth (BLD, e.g., Batchvarova & Gryning, 1991; H. Liu et al., 2001).
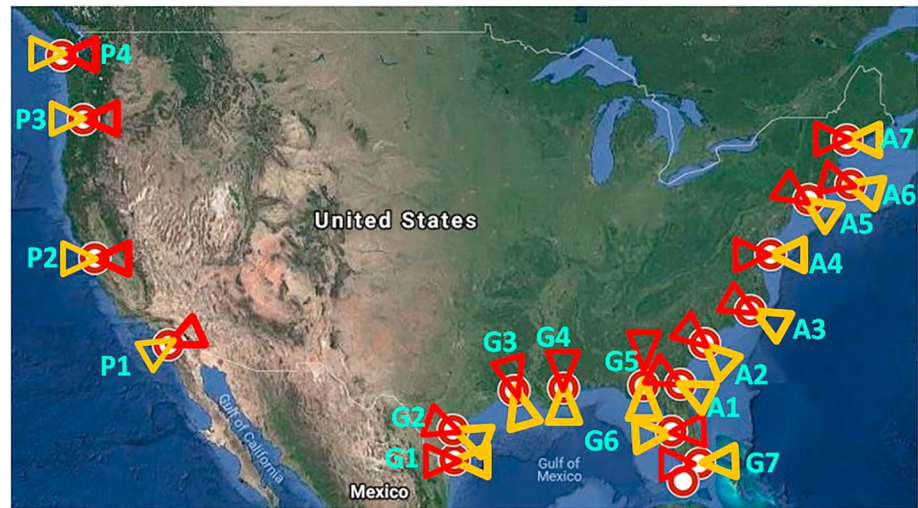
Figure 1. Locations of the 18 coastal sites in the contiguous United States along the Gulf of Mexico (seven sites, G1–G7), Atlantic Ocean (seven sites, A1–A7), and Pacific Ocean (four sites, P1–P4). Red and yellow triangles mark the offshore and onshore flows, respectively (see supporting information for further details).

Numerous research efforts were made to investigate the spatial (local to regional scale) and temporal (diurnal and seasonal time scales) BLD variability over land surface (e.g., Illingworth et al., 2018) and spatiotemporal variability of the depths of the marine boundary layer (MBL) over different oceans and seas (S. Liu & Liang, 2010). However, empirical studies for coastal regions are often limited in scope, as they were largely confined to short-term case studies or over a single coastal region (e.g., Angevine et al., 2006; Stauffer et al., 2015). Additionally, many researchers recommended the application of long-term measurements to evaluate the consistencies of the impact of onshore and offshore flows on BLDs in the coastal areas for obtaining a comprehensive understanding on the BLD variability across different seasons (e.g., Banta et al., 2011; Angevine et al., 2006; Stauffer et al., 2015). Both the interpretation of observed and simulated BLDs over coastal regions need to consider the impact of advection via onshore and offshore flows, which is the central point of this work. In this paper, we investigated 25 years of observations of rawinsonde-derived BLDs from 18 coastal sites in the contiguous United States (Figure 1) to outline the importance of advection on BLD footprints over coastal regions in all four seasons.

2. Data Sets and Methods

To estimate daily afternoon BLDs, we used regular rawinsonde datasets for the period from 1991 to 2015 available from the Integrated Global Radiosonde Archive (IGRA, Durre & Yin, 2008). We computed the daily afternoon BLDs (in meters above ground level, AGL) from the 00 UTC soundings using the approach developed by Lee and De Wekker (2016). After linearly interpolating the IGRA soundings every 100 m to resolve the uncertainties caused by coarser vertical resolutions of the soundings (Seidel et al., 2012), we computed the virtual potential temperature gradient (i.e., $\frac{\partial \theta_v}{\partial z}$) over each 100-m level, where z and θv are altitude and virtual potential temperature, respectively. We then scanned upward in each sounding, up to 400 m AGL and filtered the stable portion of the sounding (i.e., $\frac{\partial \theta_v}{\partial z} > 0$). We then determined the BLD as the height at which the bulk Richardson number (R_b) profile first exceeded 0.25 (e.g., Vogelezang & Holtslag, 1996; Seidel et al. (2010, 2012). Doing so allowed us to estimate the depth of quasi-stationary afternoon ABL, which is important in this study.

The meteorological conditions over coastal regions and differential heating of land-versus-water trigger the perfect environment in the late afternoon for BLDs to become quasi-stationary, well-mixed, and the internal boundary layer has grown to its maximum extent so that we could study the differences between BLDs under offshore and onshore flows (see supporting information for further details). We acknowledge, though, that there are uncertainties using the R_b-based approach, as pointed out, for example, by Seidel et al. (2010, 2012) particularly in cases where the ABL is stable. However, we mitigated this issue by removing the near-surface
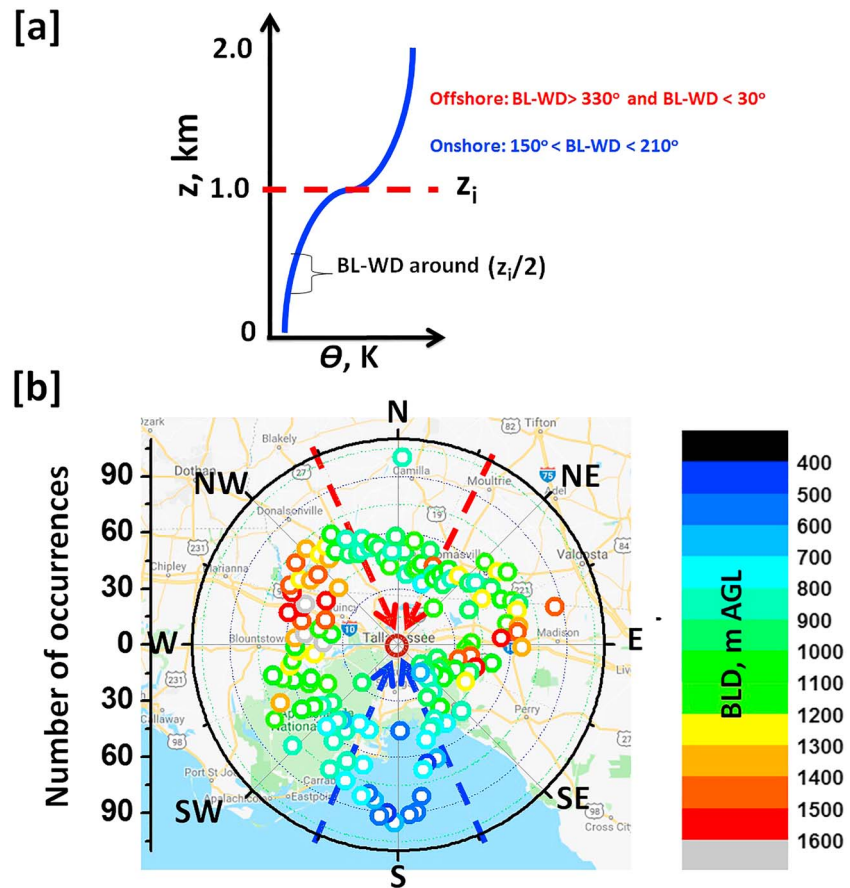
Figure 2. Estimation of BL-WD using rawinsonde profiles. The z_i is the atmospheric boundary layer top height; BL-WD marks the averaged wind direction (three-point averaged with $z_i/2$ at the center, henceforth referred as BL-WD), and θ is potential temperature (a). BLD as a function of BL-WD via frequency distribution (bin width of 2.5°) analysis of daily BL-WD for 25-year period at Tallahassee (b). Radii denote the number of occurrences and angles mark the BL-WD. Red and blue dashed arrows denote the 60° angular sectors selected for offshore and onshore flows, respectively. Colors mark the BLDs in meters above ground level (AGL). BL-WD = mean ABL wind direction; BLD = boundary layer depth.

stable layers (up to 400 m AGL) from the R_b profiles following Lee and De Wekker (2016). One of the key shortcomings of our approach is that one cannot apply this technique for growing ABL regime in the morning, as the residual layer top will be reported instead of the BLD.

Once the 25-year time series of daily afternoon BLDs were obtained, we calculated the mean ABL wind direction (BL-WD) from rawinsonde profiles of wind following the approach used in past studies (Banta et al., 2011; Berman et al., 1999; Lee & Pal, 2017; Pal & Haeffelin, 2016). Figure 2a shows a schematic of the computation of BL-WD from a thermodynamic profile, where z_i is the ABL top height and $z_i/2$ is the center of the ABL. We performed a three-point running average of raw u and v around $z_i/2$ and calculated mean wind direction at $z_i/2$ (see supporting information for similar analyses for the other sites).

To illustrate the method, we selected an arbitrary site, Tallahassee, located downwind of southerly flow of the Gulf of Mexico (G3, Figure 1). Following frequency distribution analyses of BLD as a function of BL-WD (Figure 2b), we assigned mean onshore flow regime to the BL-WD within a 60° angular sector with southerly as a center, almost orthogonal to the coast line. Thus, all the BLD samples obtained for the BL-WD of 150–210° were used to estimate the monthly median BLD for onshore flow. For offshore flows, we considered the opposite angular sector of the onshore flow (i.e., 330–30°). Sensitivity tests for different angular sectors (30°, 40°, 50°, and 60°) revealed 60° to be most appropriate so that when calculating monthly medians, we had at least five samples (i.e., 5 days) for both onshore and offshore flows. Källstrand and Smedman (1997) illustrated that fetch effect depends on BL-WD, which has high degree of variability in
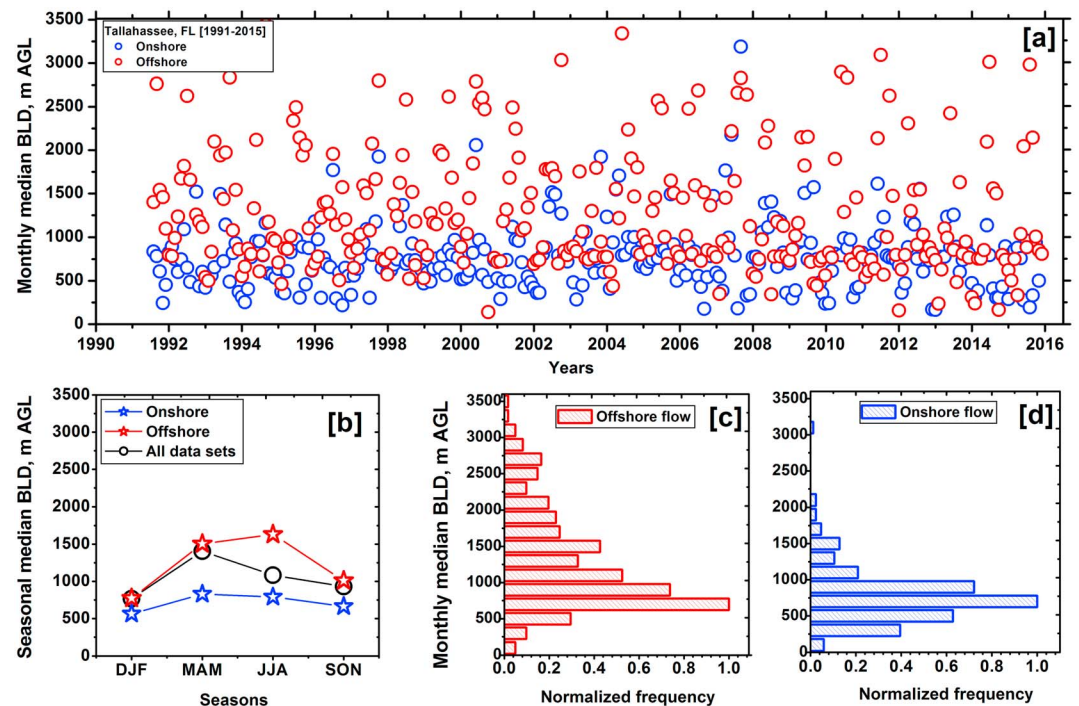
AGU
100
ADVANCING EARTH
AND SPACE SCIENCE

Geophysical Research Letters

10.1029/2018GL081699

Figure 3. Monthly median BLDs for Tallahassee for both regimes: onshore flows (blue circles) and offshore (red) flows (a). Overall seasonal cycle patterns of median BLDs for both flow regimes using 25-year climatology (b). Also overlaid is the mean seasonal cycle under all mean ABL wind direction flow regimes (black circle). Normalized frequency distributions of monthly median BLDs for offshore (c) and onshore (d) flows. BLD = boundary layer depth; AGL = above ground level.

coastal regions. Additionally, an advantage of choosing a wide angular sector (60°) for determining onshore versus offshore BL-WD samples is that errors in rawinsonde-derived wind components due to noise in rawinsonde tracking system and "pendulum" motion of the sensor in the lower altitude (Wang et al., 2009) can be considered insignificant compared to the wide angular sector (here, 60°).

3. Results and Discussion

3.1. Contrasting BLD Variability Over the Gulf Coast Site Tallahassee: An Example

We first analyzed the observed BLD variability over Tallahassee (Figure 3). Figure 3a displays the temporal variability of monthly median BLDs under both offshore (red circles) and onshore (blue circles) flows for the entire study period, suggesting more BLD variability under offshore than under onshore flows. For BLDs over Tallahassee site, under offshore flows, we found a standard deviation and interquartile range of 703 and 884 m, respectively, while for onshore flow, they were 376 and 357 m, respectively. The frequency distribution analyses for median BLDs under offshore (Figure 3c) and onshore (Figure 3d) flows show much longer-tailed distributions, with higher median for BLDs under offshore (1,039 m AGL) than the onshore (748 m AGL) flow. Also, the distribution of BLDs under offshore flows was found to be much flatter (kurtosis of 0.51) than the BLDs under onshore flows (kurtosis of 6.55).

The seasonal cycle in median BLDs under offshore flows was found to be more pronounced than under onshore flows (Figure 3b). Additionally, the pattern of the seasonal cycle of median BLDs using all available measurements (i.e., without any BL-WD sampling) lies in between the two flow regimes. Furthermore, the overall seasonal cycle pattern is either overestimated compared to onshore BLD in June–August or underestimated compared to offshore BLD in June–August. Georgoulias et al. (2009) reported a slight reduction in BLDs for onshore flows than the BLD during all summer days. We also analyzed temporal variability in the median BLDs over Tallahassee under both flows during the period 1991–2015 via box and whisker analyses for each season (see Figure S4) and identical analyses for the other 17 coastal sites (not shown).
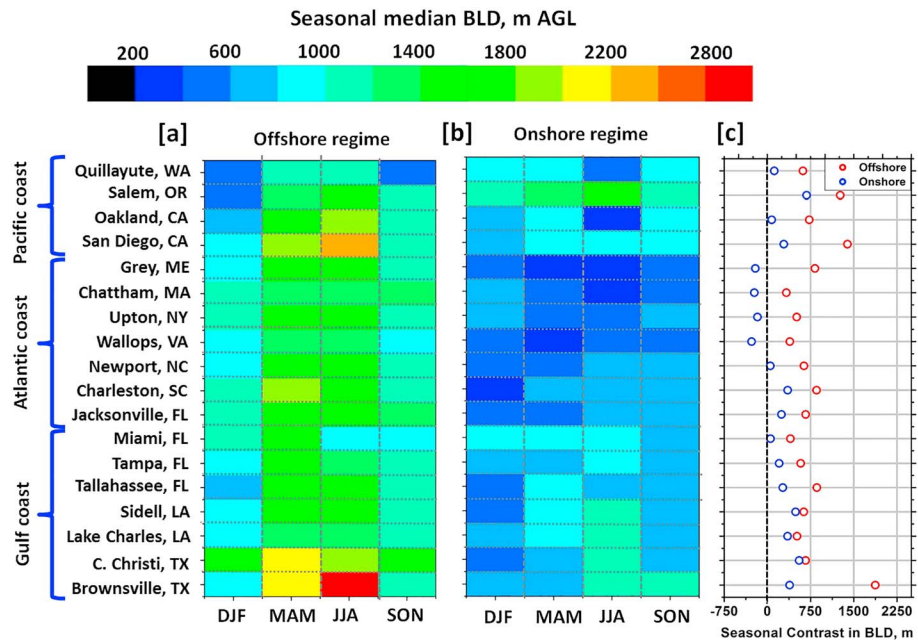
Figure 4. Climatological averaged seasonal cycle patterns of median BLDs for all the 18 sites as marked on the *y* axis. Winter: December–February (DJF); spring: March–May (MAM); summer: June–August (JJA); and fall: September–November (SON). Each pixel denotes an overall seasonal median BLD for a particular site for both offshore (a) and onshore (b) flows. Color bar scale limits vary between 200 and 2,800 m AGL. Seasonal contrast in BLDs for all the sites (c); red and blue circles mark the seasonal contrasts for offshore and onshore flows, respectively. BLD = boundary layer depth; AGL = above ground level.

3.2. BLD Seasonal Cycles Over All the Sites

Using the monthly median BLDs, we computed the seasonal BLD variability for onshore and offshore flows over the 18 sites. Site-to-site variability in the seasonal median BLDs over all sites under offshore and onshore flows is displayed in Figures 4a and 4b, respectively. Under offshore flows, BLD variability follows the well-known BLD seasonal cycle patterns typically observed over continental sites, yielding deeper ABL during spring and summer compared to winter and fall (e.g., Stull, 1988; von Engeln & Teixeira, 2013).

In contrast, BLD seasonal cycles under onshore flows for all sites do not show a clear and consistent seasonal pattern. For instance, BLD seasonal cycles over many sites, i.e., Grey, Chatham, Upton, Newport, Miami, and Quillayute, do not show any significant differences in BLDs across the four seasons under onshore flows. Overall, the observed BLD seasonal cycles under onshore flows over all sites reflect the MBL depth seasonal cycle patterns instead (e.g., de Boyer Montegut et al., 2004).

Sicard et al. (2006) found either no significant differences in BLDs between summer and winter or even lower BLDs during summer than in winter, though they did not distinguish their findings using onshore versus offshore flows. Matthias et al. (2004) also reported similar findings (i.e., lower BLDs in summer than in winter) for other coastal sites (e.g., Athens, Greece; Lecce, Italy). Additionally, Berman et al. (1999), while studying BLD variability over coastal sites in the Mid-Atlantic region, speculated that the interplay between sea-breeze circulations and synoptic-scale wind patterns was a key factor for larger BLD contrasts. Thus, the results reported here are first-of-a-kind empirical evidence of the seasonal cycles in BLD contrasts under offshore and onshore flows over three diverse coastal regions.

3.3. Seasonal Contrast in BLDs

The seasonal contrasts (often referred to as seasonal cycle amplitudes) were obtained by subtracting the seasonal scale minimum BLD (i.e., observed during winter months December–February) from the maximum BLD (i.e., observed during either summer or spring). Figure 4c shows the seasonal changes in the observed BLD for both offshore (red circles) and onshore (blue circles) flows at all the sites. For instance, seasonal contrasts in BLDs for offshore flows were found by subtracting the winter median BLD from summer median
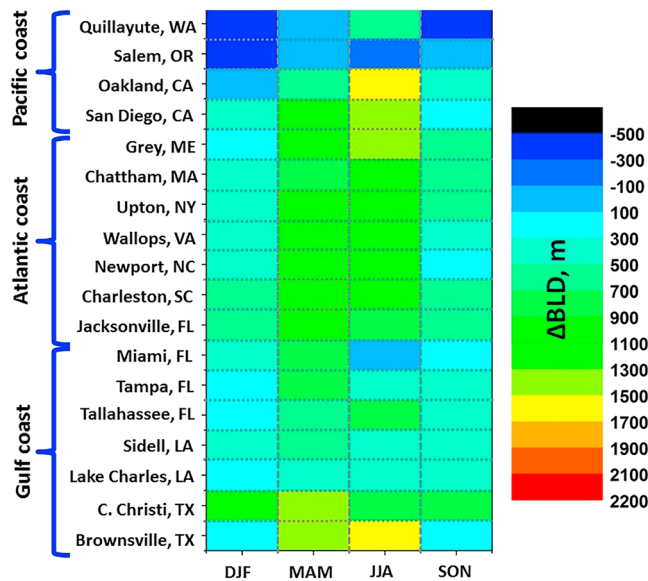
Figure 5. Overall seasonal cycles of ΔBLD for the 18 coastal sites based on a 25-year climatology. Each colored pixel marks ΔBLD in meters for an individual site during a particular season. A color bar scale (between −500 and 2,200 m) was chosen to characterize the diverse impact of contrasting flows on the atmospheric boundary layer over coastal areas during different seasons. BLD = boundary layer depth.

BLD. The zero line in Figure 4c helps determine whether or not the seasonal cycles of BLD at the coastal sites are positive or negative. A positive seasonal contrast indicates typical BLD seasonal cycle feature over land in the mid-latitudes, implying deeper BLDs in summer and spring than winter (e.g., Georgoulias et al., 2009) and vice versa for negative seasonal contrasts (e.g., McGrath-Spangler & Denning, 2013).

Figure 4c shows distinct differentiations in the seasonal cycle of BLDs under two flow regimes. In general, a relatively stronger seasonal cycle in BLD for offshore flows than for onshore flows was observed. The MBL-depths seasonality is less pronounced compared to the BLDs over land (Kara et al., 2003). Thus, the observed BLDs under onshore flows are associated with an influx of MBL air so that BLD seasonality in these conditions is also less pronounced and more representative of MBL depths. Additionally, BLD seasonal changes for offshore flows are always positive, unlike for onshore flows. The BLD seasonal contrasts vary from 200 to 1,850 m among the sites for offshore flows, while for onshore flows, the contrasts vary between −230 and 730 m. Notably, under onshore flows, BLD variabilities over Miami and Newport show almost no seasonality (seasonal contrasts ≈0 m), whereas four other sites (Wallops, Upton, Chatham, and Grey) show negative BLD seasonal contrasts. Conversely, for offshore flows, large seasonal contrasts in BLDs (>1,400 m) were found for three sites: Brownsville along the Gulf Coast and San Diego and Oakland along the Pacific Coast.

The rawinsonde observation site at Brownsville is characterized by a semi-arid climate with low precipitation. For instance, the mean summertime precipitation over 1981–2010 was 5.9 cm, and year-to-year variability was extreme with a drift of summer precipitation of around −5-4 cm. Deep ABL in summer over such climatic regions in the United States are not unusual, as reported in previous studies (Lee & Pal, 2017; Seidel et al., 2010). Both rawinsonde sites at San Diego and Oakland are characterized by urban hotspots which likely trigger high summer time BLDs under offshore flow. These results cumulatively explain that, under onshore flows, the impact of MBL on the BLD over coastal sites is substantial, consistent with previous findings (e.g., De Tomasi et al., 2011; Melas et al., 2005).

3.4. Overall BLD Contrasts for Offshore and Onshore Flows

The overall seasonal cycles of ΔBLD (seasonally median BLD under offshore minus onshore flow) show the dependencies of BLDs on the history of two different air parcels: marine air mass advected via onshore flows and continental air mass via offshore flows (Figure 5). Except for two sites along the Pacific Coast, mostly positive ΔBLDs were observed with strikingly higher ΔBLDs during summer and spring (500–1,500 m) than during winter and fall (100–450 m), illustrating the contrasts in continental ABL to coastal internal boundary layer regimes over most of the sites. Matsouka (2006) showed higher frequencies of sea breeze occurrences in summer months (up to 70% of the time) and their impact on ABL. However, a clear seasonal pattern of ΔBLDs in different seasons was absent.

For the two sites along the Gulf of Mexico (Corpus Christi and Brownsville), high ΔBLDs were observed during spring and summer, which likely indicates the impacts of deep ABLs in the southeast Texas during warm seasons. Over other sites along the Gulf of Mexico, similar ΔBLDs (≈300–500 m) were observed during summer and spring, except at Miami. Another feature is that, for two of the sites (Slidell and Lake Charles), ΔBLDs were almost invariable, with average ΔBLDs of 250 m around the year. These occur because bay areas along the complex coast line of Louisiana are narrow, so that the impact of onshore flows on the BLDs is insignificant. Most of the Atlantic Coast sites have similar patterns in the ΔBLD seasonal cycle, yielding higher ΔBLDs in spring and summer (≈1000 m) than in the fall and winter (≈350 m). These results illustrate the impact of advected MBL from Atlantic Ocean via easterly or southeasterly flows on the BLDs over the coastal sites.

Also, for the Pacific Coast sites, we found that variability in the advection via offshore and onshore flows explains significant changes in BLDs during both warm and cold seasons. During summer and spring, ΔBLD remains mainly positive like other two coastal regions. In particular, ΔBLD for San Diego and Oakland sites during summer months were found to be exceptionally high (1,100–1,300 m), likely due to the impacts of urban boundary layer and ABL features from adjacent mountains advected via offshore flow. Conversely, ΔBLD for Quillayute was found to be very low (300–400 m during warm season). ΔBLDs over these two Pacific sites yield even −300 m during the cold season, likely due to the advection of colder air masses, compared to those from over the Pacific, originating over the interior of the continent during these months. Bianco et al. (2011) attributed the shallower BLDs at four sites in California's central valley during the summer months to the onshore flows in the afternoon. Additionally, over another coastal site along the Pacific Ocean (Vancouver), van der Kamp and McKendry (2010) observed insignificant BLD growth throughout the year and attributed their findings to onshore flow, without any empirical evidence of BL-WD.

4. Conclusions

Using 25 years of rawinsonde measurements over 18 coastal sites along the three coastal regions of the contiguous United States (Gulf of Mexico, Atlantic Ocean, and Pacific Ocean), we presented a detailed investigation of the seasonal cycles of BLDs, which revealed significant contrasts between BLDs under offshore and onshore flows during four seasons. Results illustrate the impact of the MBL on the BLD footprints of the coastal areas under onshore versus offshore flows. Our study underscores the importance of considering advection of MBL air masses via onshore flows in all seasons on the BLD seasonal cycles.

An interesting seasonal pattern emerged along the Pacific Ocean with significantly higher BLD seasonal contrasts of ≈1,400 m under offshore wind conditions implying the impact of the west coast mountains in enhancing BLDs downwind. Conversely, under onshore flow conditions, BLD seasonal contrasts were lower compared to the offshore flows and similar across all the sites along the Pacific Coast. A limitation of our methodology is that it cannot be applied for studying offshore versus onshore BLD contrasts during the morning transition period when significant BLD growth occurs and the development of the internal boundary layer commences.

The results reported demonstrate novel approaches in which long-term observational resources can be used to enhance our understanding of MBL-ABL interactions. Our findings provide unique observational constraints for model evaluation and will help adjust ABL parameterization schemes. Also, results pertaining to the BLDs under contrasting flows have direct implications for optimizing onshore wind turbines, one of the key hurdles in wind energy production. In the future, we will extend our work using similar long-term BLD observations over other coastal sites around the world.

References

Angevine, W. M., Tjernstrom, M., & Zagar, M. (2006). Modeling of the coastal boundary layer and pollutant transport in New England. *Journal of Applied Meteorology and Climatology*, *45*(1), 137–154. https://doi.org/10.1175/JAM2333.1

Banta, R. M., Senff, C. J., Alvarez, R. J., Langford, A. O., Parrish, D. D., Trainer, M. K., et al. (2011). Dependence of daily peak O_3 concentrations near Houston, Texas, on environmental factors: Wind speed, temperature, and boundary-layer depth. *Atmospheric Environment*, *45*(1), 162–173. https://doi.org/10.1016/j.atmosenv.2010.09.030

Batchvarova, E., & Gryning, S. E. (1991). Applied model for the growth of the daytime mixed layer. *Boundary-Layer Meteorology*, *56*(3), 261–274. https://doi.org/10.1007/BF00120423

Behrendt, A., Wagner, G., Petrova, A., Shiler, M., Pal, S., Schaberl, T., & Wulfmeyer, V. (2005). Modular lidar systems for high-resolution 4-dimensional measurements of water vapor, temperature, and aerosols. In U.N. Singh & K. Mizutani (Eds.), *Lidar remote sensing for industry and environment monitoring V, Proceedings of SPIE 5653* (pp. 220–227). Honolulu, HI.

Berman, S., Ku, J. -Y., & Rao, S. –T. (1999). Spatial and temporal variation in the mixing depth over the northeastern United States during the summer of 1995. *Journal of Applied Meteorology*, *38*(12), 1661–1673. https://doi.org/10.1175/1520-0450(1999)038<1661:SATVIT>2.0.CO;2

Bianco, L., Djalalova, I. V., King, C. W., & Wilczak, J. M. (2011). Diurnal evolution and annual variability of boundary-layer height and its correlation to other meteorological variables in California's Central Valley. *Boundary Layer Meteorology*, *140*(3), 491–511. https://doi.org/10.1007/s10546-011-9622-4

Davy, R., & Esau, I. (2016). Differences in the efficacy of climate forcings explained by variations in atmospheric boundary layer depth. *Nature Communications*, *7*(1), 2016. https://doi.org/10.1038/ncomms11690

de Boyer Montegut, C., Madec, G., Fischer, A. S., Lazar, A., & Iudicone, D. (2004). Mixed layer depth over the global ocean: An examination of profile data and a profile-based climatology. *Journal of Geophysical Research*, *109*, C12003. https://doi.org/10.1029/2004JC002378

De Tomasi, F., Miglietta, M., & Perrone, M. R. (2011). The growth of the planetary boundary layer at a coastal site: A case study. *Boundary Layer Meteorology*, *139*(3), 521–541. https://doi.org/10.1007/s10546-011-9592-6

Durre, I., & Yin, X. (2008). Enhanced radiosonde data for studies of vertical structure. *Bulletin of the American Meteorological Society*, *89*(9), 1257–1262. https://doi.org/10.1175/2008BAMS2603.1

Georgoulias, A. K., Papanastasiou, D. K., Melas, D., Amiridis, V., & Alexandri, G. (2009). Statistical analysis of boundary layer height in suburban environment. *Meteorology and Atmospheric Physics*, *104*(1-2), 103–111. https://doi.org/10.1007/s00703-009-0021-z

Illingworth, A. J., Cimini, D., Haefele, A., Haeffelin, M., Hervo, M., Kotthaus, S., et al. (2018). How can existing ground-based profiling instruments improve European weather forecasts? *Bulletin of American Meteorological Society*. https://doi.org/10.1175/BAMS-D-17-0231.1

Källstrand, B., & Smedman, A. S. (1997). A case study of the near-neutral coastal internal boundary layer growth: Aircraft measurements compared with different model estimates. *Boundary Layer Meteorology*, *85*(1), 1–33. https://doi.org/10.1023/A:1000475315106

Kara, A. B., Rochford, P. A., & Hurlburt, H. E. (2003). Mixed layer depth variability over the global ocean. *Journal of Geophysical Research*, *108*(C3), 3079. https://doi.org/10.1029/2000JC000736

Lee, T. R., & De Wekker, S. F. J. (2016). Estimating daytime planetary boundary layer heights over a valley from rawinsonde observations at a nearby airport: An application to the Page Valley in Virginia, USA. *Journal of Applied Meteorology and Climatology*, *55*(3), 791–809. https://doi.org/10.1175/JAMC-D-15-0300.1

Lee, T. R., & Pal, S. (2017). On the potential of 25 years (1991–2015) of rawinsonde measurements for elucidating climatological and spatiotemporal patterns of afternoon boundary layer depths over the contiguous US. *Advances in Meteorology*, *2017*, 1–19. https://doi.org/10.1155/2017/6841239

Liu, H., Chan, J. C. L., & Chang, A. Y. S. (2001). Internal boundary layer structure under sea-breeze conditions in Hong Kong. *Atmospheric Environment*, *35*(4), 683–692. https://doi.org/10.1016/S1352-2310(00)00335-6

Liu, S., & Liang, X. Z. (2010). Observed diurnal cycle climatology of planetary boundary layer height. *Journal of Climate*, *23*(21), 5790–5809. https://doi.org/10.1175/2010JCLI3552.1

Marshall, C. H., Pielke, R. A. Sr., Stayaert, L. T., & Willard, D. A. (2004). The impact of anthropogenic land-cover change on the Florida Sea breezes and warm season sensible weather. *Monthly Weather Review*, *132*(1), 28–52. https://doi.org/10.1175/1520-0493(2004)132<0028:TIOALC>2.0.CO;2

Matsouka, I. (2006). *The impact of the sea breeze on pollution levels in Thessaloniki*. Aristotle University of Thessaloniki, Master Thesis. Thessaloniki, Greece: School of Physics, Faculty of Sciences.

Matthias, V., Balis, D., Bösenberg, J., Eixmann, R., Iarlori, M., Komguem, L., et al. (2004). Vertical aerosol distribution over Europe: Statistical analysis of raman lidar data from 10 European aerosol research lidar network (EARLINET) stations. *Journal of Geophysical Research*, *109*, D18201. https://doi.org/10.1029/2004JD004638

McGrath-Spangler, E. L., & Denning, A. S. (2013). Global seasonal variations of midday planetary boundary layer depth from CALIPSO space-borne LIDAR. *Journal of Geophysical Research: Atmospheres*, *118*, 1226–1233. https://doi.org/10.1002/jgrd.50198

Medeiros, B., Hall, A., & Stevens, B. (2005). What controls the mean depth of the PBL? *Journal of Climate*, *18*(16), 3157–3172. https://doi.org/10.1175/JCLI3417.1

Melas, D., Kioutsioukis, I., & Lazaridis, M. (2005). The impact of sea breeze on air quality in Athens. In I. Farago, et al. (Eds.), *Advances of air pollution modelling for environmental security* (pp. 285–296). Dordrecht, Netherlands: Springer. https://doi.org/10.1007/1-4020-3351-6_26

Neumann, B., Vafeidis, A. T., Zimmermann, J., & Nicholls, R. J. (2015). Future coastal population growth and exposure to sea-level rise and coastal flooding—A global assessment. *PLoS One*, *10*(3), e0118571. https://doi.org/10.1371/journal.pone.0118571

Pal, S., & Haeffelin, M. (2016). Forcing mechanisms governing diurnal, seasonal, and inter-annual variability in the boundary layer depths: five years of continuous lidar observations over a suburban site near Paris. *Journal of Geophysical Research: Atmospheres*, *120*, 11,936–11,956. https://doi.org/10.1002/2015JD023268

Pichugina, Y. L., Banta, R. M., Brewer, W. A., Sandberg, S. P., & Hardesty, R. M. (2012). Doppler lidar-based wind-profile measurement system for offshore wind energy and other marine boundary layer applications. *Journal of Applied Meteorology and Climatology*, *51*, 327–349.

Seidel, D. J., Ao, C. O., & Li, K. (2010). Estimating climatological planetary boundary layer heights from radiosonde observations: Comparison of methods and uncertainty analysis. *Journal of Geophysical Research*, *115*, D16113. https://doi.org/10.1029/2009JD013680

Seidel, D. J., Zhang, Y., Beljaars, A., Golaz, J.-C., Jacobson, A. R., & Medeiros, B. (2012). Climatology of the planetary boundary layer over the continental United States and Europe. *Journal of Geophysical Research.*, *117*, D17106. https://doi.org/10.1029/2012JD018143

Sicard, M., Perez, C., Rocadenbosch, F., Baldasano, J. M., & Garcia-Vizcaino, D. (2006). Mixed-layer depth determination in the Barcelona coastal area from regular lidar measurements: Methods, results and limitations. *Boundary Layer Meteorology*, *119*(1), 135–157. https://doi.org/10.1007/s10546-005-9005-9

Stull, R. B. (1988). *An introduction to boundary layer meteorology* (p. 666). Dordrecht, Netherlands: Kluwer Academic Publishers. https://doi.org/10.1007/978-94-009-3027-8

Stauffer, R. M., Thompson, A. M., Martins, D. K., Clark, R. D., Goldberg, D. L., Loughner, C. P., et al. (2015). Bay breeze influence on surface ozone at Edgewood, MD during July 2011. *Journal of Atmospheric Chemistry*, *69*, 1–19. https://doi.org/10.1007/s10874-012-9241-6

van der Kamp, D., & McKendry, I. (2010). Diurnal and seasonal trends in convective mixed-layer heights estimated from two years of continuous ceilometer observations in Vancouver, BC. *Boundary-Layer Meteorology*, *137*(3), 459–475. https://doi.org/10.1007/s10546-010-9535-7

Vogelezang, D. H. P., & Holtslag, A. A. M. (1996). Evaluation and model impacts of alternative boundary-layer height formulations. *Boundary-Layer Meteorology*, *81*(3-4), 245–269. https://doi.org/10.1007/BF02430331

von Engeln, A., & Teixeira, J. (2013). A planetary boundary layer height climatology derived from ECMWF reanalysis data. *Journal of Climate*, *26*(17), 6575–6590. https://doi.org/10.1175/JCLI-D-12-00385.1

Wang, J., Bian, J., Brown, W. O., Cole, H., Grubišić, V., & Young, K. (2009). Vertical air motion from T-REX radiosonde and dropsonde data. *Journal of Atmospheric and Oceanic Technology*, *26*(5), 928–942. https://doi.org/10.1175/2008JTECHA1240.1